

SWIMMING IN THE PTEROPOD MOLLUSC, *CLIONE LIMACINA*

I. BEHAVIOUR AND MORPHOLOGY*

By RICHARD A. SATTERLIE

Department of Zoology, Arizona State University, Tempe, Arizona 85287, U.S.A.

MICHAEL LABARBERA

Department of Anatomy, University of Chicago, Chicago, Illinois 60687, U.S.A.

AND ANDREW N. SPENCER

Department of Zoology, University of Alberta, Edmonton, Alberta, Canada T6G 2E9

Accepted 25 October 1984

SUMMARY

In the pteropod mollusc *Clione limacina* (Phipps), swimming is accomplished through alternate dorsal and ventral flexions of a pair of strongly muscularized wing-like parapodia (wings). Wing musculature is arranged in seven muscle groups. The two outermost dorsal and ventral groups produce the bending movements of swimming. The three inner muscle groups include longitudinal and transverse wing retractors and dorso-ventral muscles. The overall muscle arrangement is similar to that of the generalized mollusc foot.

During hovering locomotion the wings pronate on downstroke and supinate on upstroke to produce a maximal angle of attack of 42° for both phases. Wing tips nearly touch or overlap in the sagittal plane at the extreme of each half-cycle. High speed movie analysis of hovering swimming indicates that upstroke and downstroke are nearly symmetrical. It is suggested that wings produce lift in both wing phases.

We estimate from wing dimensions and velocity measurements that the Reynolds number of the wings is approximately 200. A novel lift-generating mechanism, similar to the 'clap-and-fling' of insects, may be utilized by the *Clione* wing to generate lift throughout the wing cycle despite the reversal of wing movement in each half-stroke.

INTRODUCTION

Swimming has been described for many opisthobranch molluscs both behaviourally and neurophysiologically (i.e. Morton, 1958; Willows, 1967; Willows & Hoyle, 1969; Farmer, 1970; Hughes, 1971; Weevers, 1971; Bebbington & Hughes,

*A significant portion of this work was conducted at Friday Harbor Laboratories, Friday Harbor, Washington.

Key words: Locomotion, swimming, parapodial musculature.

1973; Willows, Dorsett & Hoyle, 1973; Hamilton & Ambrose, 1975; Willows & Dorsett, 1975; Getting, 1977, 1981, 1982; Von der Porten, Redmann, Rothman & Pinsker, 1980). Swimming opisthobranchs have provided excellent opportunities for examining the cellular basis of pattern generation underlying rhythmic behaviour. Many forms of opisthobranch swimming have been described including alternate lateral flexions of the body, alternate dorsal and ventral flexions of the body, flapping or undulation of parapodia, or rowing movements of cerata (Farmer, 1970). In the gymnosomatous pteropods, including *Clione limacina*, the foot is reduced and the parapodia are highly modified, taking the form of muscularized, lateral wings. Gymnosomes are excellent swimmers using a sculling motion of the wings to provide forward propulsion during both the wing upstroke (dorsal flexion) and downstroke (ventral flexion; Morton, 1958).

Gymnosomes have presumably lost all contact with the substratum and are exclusively planktonic; their swimming is too weak to counteract the effects of currents. Swimming is a continuous or regular form of locomotion rather than a triggered response as in many opisthobranchs (i.e. *Tritonia*; Willows, 1967; Willows & Hoyle, 1969). In the pteropods it is possible to examine a fairly simple rhythmic and spontaneous behaviour, from the mechanical and hydrodynamic properties of the structures involved to the underlying cellular activity of neuronal and muscular elements producing the behaviour. In addition, comparisons can be made between hovering and swimming in *Clione* and the hovering flight of insects and birds, particularly those insects which use novel aerodynamic techniques for generating lift to overcome the effects of viscosity and drag, problems associated with propulsion at low Reynolds number (Weis-Fogh, 1973, 1975).

The purpose of this paper is to provide a description of hovering swimming in *Clione* to form a foundation for current work on the neurophysiological control of parapodial movements (Satterlie & Spencer, 1985), and the energetics and biomechanics of swimming in these animals.

MATERIALS AND METHODS

Actively swimming specimens of *Clione*, up to 2 cm in length, were dipped from waters off the dock at Friday Harbor Laboratories and held in large beakers partially submerged in a sea table at 10–13°C. Beaker water was changed once to twice daily. Healthy animals were filmed with a Redlake Locam high speed ciné camera by using Kodak Plus-X motion picture negative film. Two filming arrangements were used. The oral view (Fig. 5) was obtained filming from above at 150 frames s⁻¹ with the animals allowed to hover normally in a small finger bowl of sea water. Animals were filmed when they were at least one-half body length from the bottom of the bowl. Microscope lamps were used for side illumination. No attempt was made to regulate temperature in the oral view films. For side-view filming, animals were placed in a 10×15×15 cm glass photographic chamber immersed in a second chamber around which cool sea water was circulated. The animals were allowed to swim freely while being filmed from the side at 100 frames s⁻¹. In most lateral films, animals were slowly

swimming forward (upward). Photo-flood lamps were used for illumination, primarily from above. Films were analysed frame-by-frame by projecting the film onto a white wall with a slide projector. Tracings or measurements were made from the projected images. Angles of attack were measured as the plane of the wing at midline crossover relative to the anterior-posterior axis of the body. Photographs were printed directly from the oral-view film (Fig. 5), however, for clarity, 35 mm photographs in side view are presented to show different phases of the wing beat (Fig. 8). The 35 mm photographs were taken in the same cooled tank as the side view movies. A Nikon FM camera with a 55 mm MicroNikkor lens was used; illumination came from a Vivitar 283 electronic strobe. All photos were shot at F22–32 on Plus-X Film.

Specimens used for histological examination were relaxed in a 1:1 mixture of sea water and isotonic MgCl_2 (0.33 mol l^{-1}) and fixed for 48 h in Bouin's fixative or 10% formaldehyde in sea water. Following dehydration and paraffin embedding, the tissue was cut at 10–15 μm and stained according to the One-Step Trichrome technique of Gabe (1976). The wing section in Fig. 2 was cut by hand from a plastic block following fixation in cacodylate-buffered glutaraldehyde (2%) and osmium tetroxide (1%). The thick section was not stained.

RESULTS

The body of *Clione limacina* is roughly torpedo-shaped with a somewhat blunt head and tapered tail (Fig. 1). Mantle cavity and gills are absent. A pair of retractile tentacles project from the head. Set back approximately one-quarter of the body length, on the dorsal side, are a pair of cephalic tentacles which bear rudimentary eyes (Hyman, 1967). Slightly posterior to the cephalic tentacles are a pair of laterally projecting, strongly muscularized wing-like parapodia. The sites of wing attachment to the body are not on the dorso-ventral midline, but rather are slightly displaced ventrally. Forward locomotion, which is almost exclusively in a vertical orientation and directed towards the water surface, results from alternating flexions of the parapodia (wings) in the morphologically dorsal and ventral directions.

'Wing' structure

Wing length (base-to-tip) can exceed 5 mm in large specimens, with a chord of over 4.5 mm at the widest point (maximum chord occurs at approximately one-third wing length, measured from the body). Wing thickness, measured from a relaxed wing of a large specimen, is 250 μm near the point of attachment to the body, and decreases slightly toward the wing tip. Cut in a plane parallel to the long axis of the body, the wing is thickest posterior to the leading edge and tapers to a point at the trailing edge (Fig. 2). The wings are flexible throughout their length and chord when the musculature is relaxed.

Seven distinct groups of muscle bundles can be identified in the wing. The 'swimming' muscles include four laminae of bundles, two each associated with the

dorsal and ventral surfaces of the wing (Figs 2, 3, 4). For each surface, the outermost muscle layer, immediately underlying the surface epithelium together with a thin layer of subepithelial connective tissue, consists of fibres orientated obliquely to the long axis of the body, with points of attachment at the distal anterior margin and proximal posterior margin of the wing (Fig. 4). These dorsal and ventral anterior oblique muscles (named for their attachment to the anterior free edge of the wing) form continuous sheets of parallel bundles across the wing (Figs 2, 3). Each muscle layer is one bundle thick. The muscle bundles are 45–90 μm in diameter and each includes up to 30 muscle cell profiles in cross section. Immediately inside each anterior oblique layer is a similar layer of parallel bundles which lie nearly perpendicular to the anterior obliques (Fig. 3). The two muscle sheets cross at an angle of 105° (Fig. 4). The inner muscle bundles attach at the proximal anterior margin and distal posterior margin of the wing, and are therefore termed dorsal and ventral posterior oblique muscles.

Separating the dorsal and ventral swimming muscle groups is a haemocoelic space (Figs 2, 3), averaging 100 μm across, in which the remaining three muscle groups and the main nerves innervating the wing are found. Two of these muscle groups are

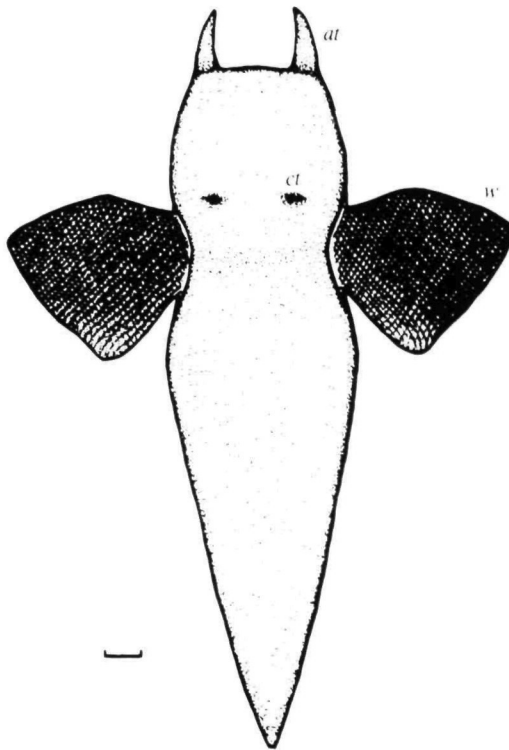


Fig. 1. *Clione limacina*. Scale drawing of a large preserved specimen (dorsal view, partially relaxed prior to fixation). at, anterior tentacles; cl, cephalic tentacles; w, wings. Scale bar, 1 mm.

involved in wing retraction. The transverse wing retractors extend from the body to the free edge of the wing (Fig. 3) in the form of isolated bundles (up to $50\text{ }\mu\text{m}$ in diameter) that can be traced into the body and through to the opposite wing. Longitudinal retractor muscles run perpendicular to the transverse retractors and parallel to the longitudinal body axis in bundles of dimensions similar to those of swimming muscle bundles (Fig. 2). During wing retraction, the transverse retractors pull the free edge of the wing into the body while the longitudinal retractors compress the wing in the anterior-posterior plane.

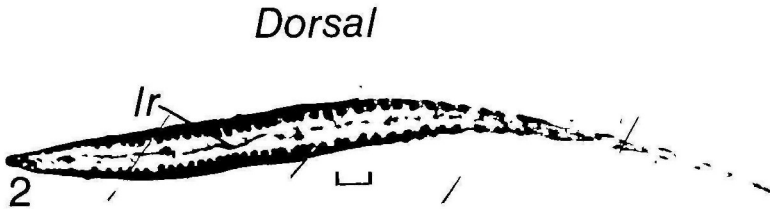


Fig. 2. Longitudinal hand-cut section of a *Clione* wing. The dorsal and ventral swimming muscles (obliques) are closely apposed to the surface epithelium. Within the central haemocoelic space are longitudinal retractor muscles (*lr*). Scale bar, $200\text{ }\mu\text{m}$.

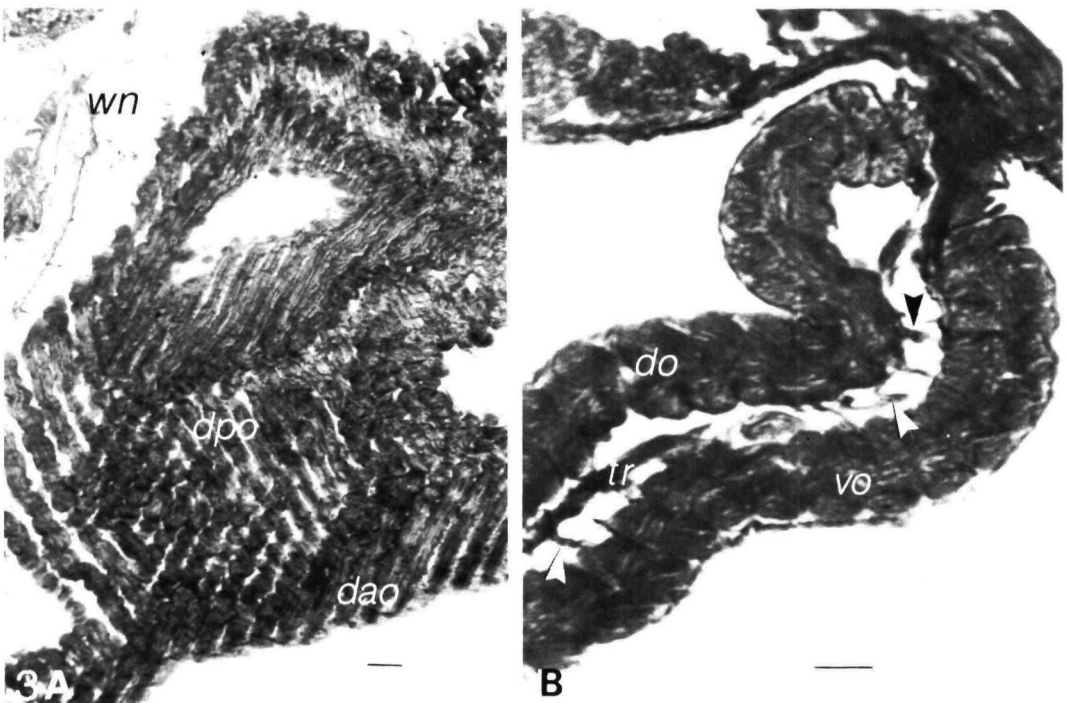


Fig. 3. (A) Tangential section of wing showing oblique muscles. Each layer is made up of tightly packed muscle bundles. *dao*, dorsal anterior obliques; *dpo*, dorsal posterior obliques; *wn*, branch of main wing nerve. (B) Longitudinal section of a wing showing dorsal (*do*) and ventral (*vo*) oblique muscle layers, transverse retractors (*tr*) and dorso-ventral muscle cells (arrows). Scale bars, (A) $100\text{ }\mu\text{m}$, (B) $50\text{ }\mu\text{m}$.

The final group of wing muscles consists of individual, stellate-shaped cells that span the haemocoel, sending multiple processes between muscle bundles of the dorsal and ventral swimming muscle layers (Fig. 2). These dorso-ventral muscles presumably control wing thickness by antagonizing increases in haemocoelic pressure which would tend to thicken the wing, and may be involved in wing protraction.

Wing movements during normal swimming

Swimming activity varied in natural and laboratory situations from hovering to fast forward locomotion at speeds of up to 10 cm s^{-1} . The following description of wing movements refers only to animals observed during hovering or slow forward (upward) swimming.

All animals observed *in situ* were actively hovering or swimming forward (upward) with a *vertical body orientation*, head uppermost, and with a wing-beat frequency of between 1 and 3 Hz. *Clione* is negatively buoyant and must swim vertically to remain at the same level in the water column. Mean sinking rates, measured in a small glass tank, ranged from 1 cm s^{-1} for animals sinking head first with the wings retracted, to 0.7 cm s^{-1} for head-first sinking with the wings expanded. Most often, sinking was terminated after a few seconds with a dorsal or ventral bend of the tail associated with full wing expansion, resulting in a glide to a horizontal attitude. When a horizontal position was attained, flapping wing movements resumed with the tail still bent, bringing the animal back to its normal, vertical orientation.

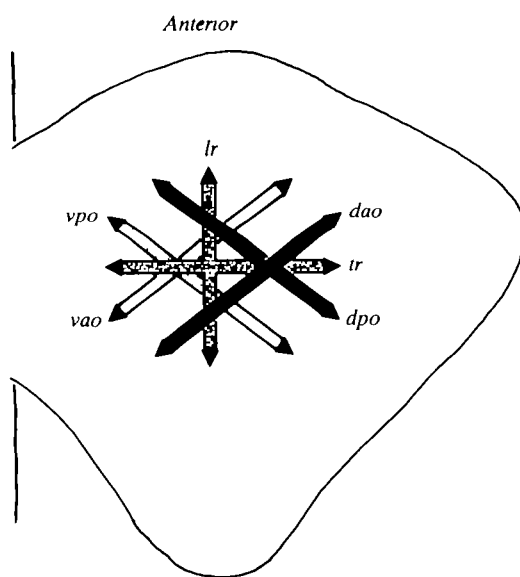


Fig. 4. Wing diagram to show orientation of muscle groups. Darkest to lightest bars indicate dorsal-most to ventral-most position. The dorso-ventral muscles (not shown) run perpendicular to the plane of the diagram. *dao*, dorsal anterior obliques; *dpo*, dorsal posterior obliques; *vpo*, ventral posterior obliques; *vao*, ventral anterior obliques; *lr*, longitudinal retractors; *tr*, transverse retractors.

Wing movements during hovering consist of alternating bilaterally coordinated dorsal and ventral flexions of the wings. At the extreme of each half-cycle of the wing beat, the wing tips nearly touch or slightly overlap in the sagittal plane (as viewed from above, Fig. 5). Wing movement involves bending of the wing throughout its length rather than a simple rotation at the point of attachment. As viewed from above, wing movements appear nearly symmetrical with respect to upstroke and downstroke (Fig. 5).

Based on film analysis of hovering swimming, the wing-beat cycle can be separated into five more-or-less distinct phases. Since the morphological upstroke (dorsal flexion) and downstroke (ventral flexion) are similar, only the latter will be discussed in detail. The cycle begins with both wing tips at the dorsal midline immediately prior to downstroke (designated 0°; Fig. 6, frame 20). In the following, 'flattening' and 'curvature' refer to changes in shape along the proximal-distal plane of the wing (most conveniently seen by observing the leading edge); 'pronation' and 'supination' refer to twisting of the plane of the wing (most easily observed from the side), to alter the angle of attack.

The initial phase of wing movement involves *flattening* of the wing (decrease in wing curvature), presumably representing the initiation of contraction of the ventral

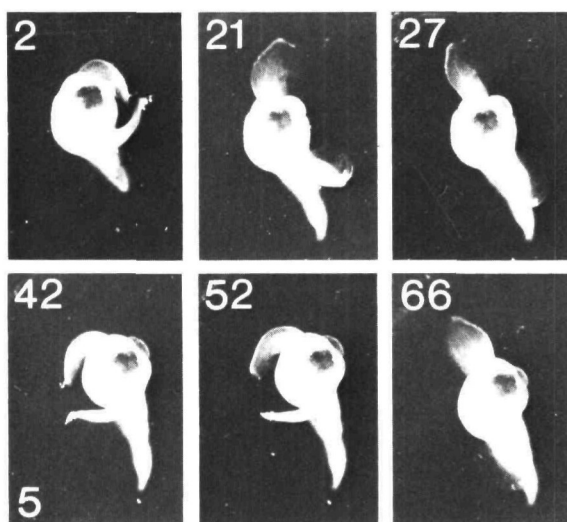


Fig. 5. Anterior view of hovering *Clione*, from ciné film (shot at 150 frames s^{-1}). Prints represent frames 2, 21, 27, 42, 52 and 66 in a series comprising a single full wing stroke. (2) End of downstroke (note wing tips nearly overlap). (21) Supination phase – wings are nearly fully supinated. (27) Wing crossover of morphological upstroke. The wings are fully supinated and the leading edge nearly straight. (42) Tip-forward phase of morphological downstroke. At this time the wing tips are moving apart and forward (anteriorly). (52) Beginning of stiffening phase. Wings continue to stiffen and begin to pronate. At this time, the wing tips are still moving forward. (66) Wing crossover of downstroke. Comparison with frame 27 shows the similarity of upstroke and downstroke. Photos are approximately three times life size. The buccal apparatus appears as a dark spot in the photos. Time of each frame; 2 = 13 ms; 21 = 140 ms; 27 = 180 ms; 42 = 280 ms; 52 = 347 ms; 66 = 440 ms. Dorsal side of body is to the left.

oblique muscles. This flattening marks the beginning of the power stroke and the initiation of wing pronation (see Fig. 7). The duration of the flattening phase is between 60 and 70 ms (frames 20–27 in Fig. 6; also see Figs 7, 8C). During this phase, the wing shape changes from an 'S' bend formed at the termination of the upstroke to a gradually straightening 'C' bend with the convex face on the ventral side (Fig. 7 positions 1–6). The wing tip, as viewed from above, begins to move away from the dorsal midline of the animal (Fig. 9). The *pronation* phase involves wing twisting to decrease the angle of attack and a ventral and slightly posterior movement of the wing tip (Fig. 10). This phase includes a continued straightening of the leading edge of the wing and lasts approximately 50 ms (frames 27–32 in Fig. 6).

During wing *crossover* (90° wing angle relative to the body), the wing tip crosses the lateral midline of the body (frame 34 in Fig. 6; see also Figs 5, 7, 8) as the wing achieves maximum pronation (Figs 5, 6, 8F,G). The angle of attack during this phase is approximately 42° for both upstroke and downstroke (upstroke, mean = $42.4 \pm 6.8^\circ$, $N = 23$; downstroke, mean = $42.5 \pm 5.2^\circ$, $N = 23$). During *crossover*, the wing tip velocity reaches a maximum value (for hovering swimming) approaching 0.1 ms^{-1} . The crossover phase lasts approximately 20–40 ms (frames 30–34 in Fig. 6). Wing flattening continues through the crossover phase, reaching a maximum, straight configuration just after midline crossover (Fig. 7 position 22,

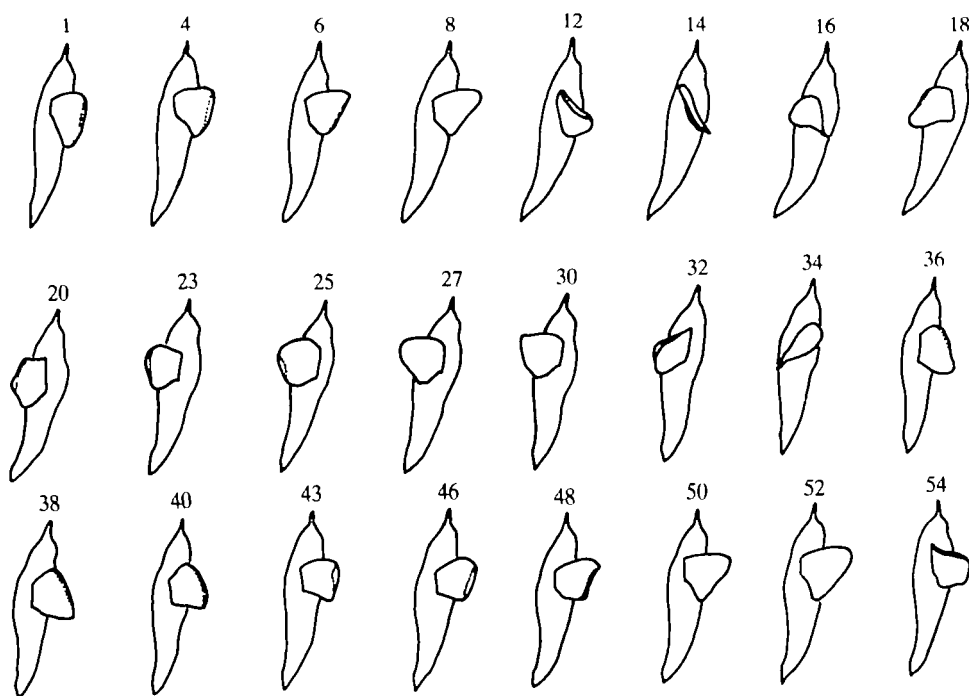


Fig. 6. Tracings of ciné frames taken in side view. One full stroke is shown. Frame numbers are indicated (filmed at $100 \text{ frames s}^{-1}$). Broken lines indicate where wing tips are hidden by remainder of wing. For frame times (in ms) multiply the frame numbers by ten. Note that the number of frames between each illustrated frame is not constant.

Fig. 9). Termination of the crossover phase represents the beginning of the transition between powerstroke and recovery as noted by the cessation of wing flattening and a gradual increase in wing flexibility (Figs 6, 7 position 29). The *flexible* phase involves a continuation of wing tip movement in a ventral, posterior direction (Fig. 10), and lasts 70–80 ms. The flexible phase ends with the wings achieving their maximal ventral bend, and the leading edges curved to form 'S' shaped profiles (frames 38–43 in Fig. 6; see also Fig. 7 position 38). The final phase of recovery, *tip-forward*, runs into the beginning of the flattening phase of upstroke, and involves the forward movement of the wing tip while the wing is in the fully curved position (frames 43–48 in Fig. 6; also see Figs 5, 10). At the end of tip-forward (180° phase), the flattening phase of the upstroke, with the resultant initiation of supination, begins. The succeeding phases of the upstroke are similar to those of the downstroke (see Figs 6, 9, 10). Note that wing curvature and wing pronation (or supination) are out of phase; maximum curvature occurs at a time of minimum pronation, and *vice versa*.

Viewed from the side, the path traced by successive wing tip positions is a horizontal figure-of-eight with a stroke plane orientated approximately perpendicular to the longitudinal body axis (Fig. 10). The angle of tilt of the wing tip path relative to the stroke plane is between 15 and 20° . The dorsal and ventral notches in the curve begin when the curvature of the wing is maximal and the wing tips are at their posterior-most position, near the dorsal or ventral midline. From there, the wing tips

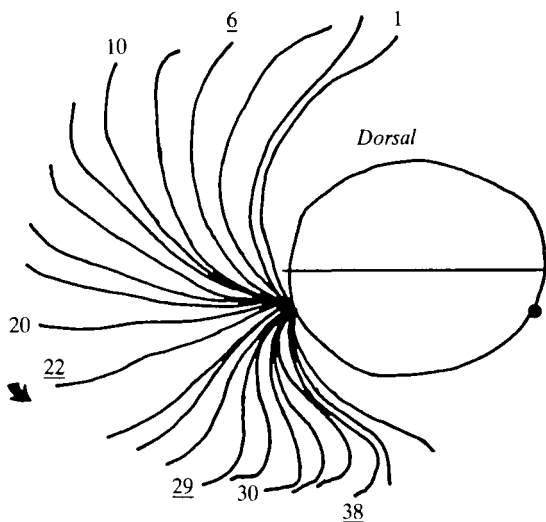


Fig. 7. Superimposed tracings of wing leading edge (as viewed from above) during morphological downstroke. Not all frames are represented. Wing length is not accurate since the entire length of the leading edge was not clear in all frames. Note the continual stiffening of the wing through wing crossover and the development of a subsequent 'S'-bend (as expected if movement is passive). Horizontal line indicates approximate location of body midline. Closed circle shows the attachment site of the other wing. Dorsal surface is uppermost. Numbers indicate frame numbers ($150 \text{ frames s}^{-1}$). Underlined numbers are referred to in the text.

move forward (tip-forward phase) while the wing itself is still maximally curved (see Fig. 6). The beginning of the next half-stroke involves wing stiffening, shown as the dorsal or ventral movement of the wing tips, which terminates the notches. Note that the figure-of-eight curve is not symmetrical, but rather is displaced ventrally. The wings are attached to the body close to the ventral surface, thus presumably influencing the wing tip curve.

Wing retraction

Wings can be totally withdrawn into the body either unilaterally or bilaterally. Mechanical stimuli, such as a repeated touch to the wing tip or head, initiate twitch-

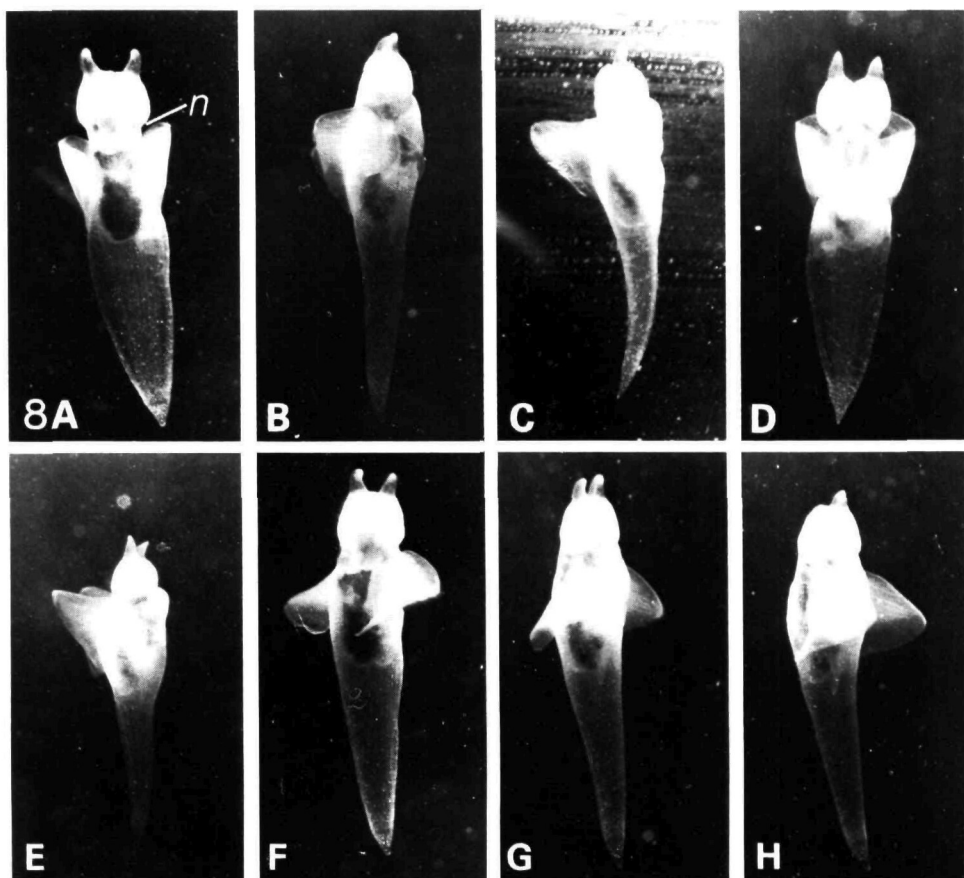


Fig. 8. Individual 35 mm photos of hovering *Clione*. All photos are not of the same animal. (A) Dorsal view at the beginning of tip forward phase. Note that the wing tips are posterior to the 'neck' region of the body (*n*). (B) Side view (dorsal to left), similar to that in A. (C) Side view of flattening phase. Note that the wing is straightened relative to B and the wing tips are nearly in line with the neck. (D) Ventral view of stage similar to C. The reduced foot can be seen. (E) Side view (dorsal to left), beginning of pronation phase. Note that the wing tip has moved forward relative to D. (F, G) Dorso-lateral and ventro-lateral views of wing crossover respectively. The wings are maximally pronated. (H) Ventro-lateral view at beginning of flexible phase. Wing tips are well posterior of neck. Photos are approximately three times life size.

like retraction movements. Once initiated, full retraction is achieved in 1–2 s. Wing tips appear to be the area most sensitive to mechanical stimulation in triggering unilateral retractions, while the head is most sensitive for bilateral retractions. A touch to the tail typically results in an increase in swimming speed. During a full retraction, the wing is deflated, presumably by the expulsion of fluid from the haemocoelic space of the wing, and compressed transversely and longitudinally by the retractor muscles. Swimming movements are inhibited during retraction movements and full wing withdrawals.

Wing expansion is slow, usually lasting several seconds, and involves an obvious inflation of the wing. Weak dorsal and ventral swimming contractions typically begin long before the wing is fully expanded, and are occasionally observed prior to the initiation of expansion.

Turning behaviour

We have been unable to determine if turning involves a change in wing movements. However, in both field and laboratory situations, the tail bends during a turn. The body wall of the tail contains well developed bundles of longitudinal muscle that are presumably used to curl the rudder-like tail.

DISCUSSION

Unlike many opisthobranchs, swimming in pteropods appears to be a continuous, spontaneous activity. External stimuli are not necessary to initiate swimming in

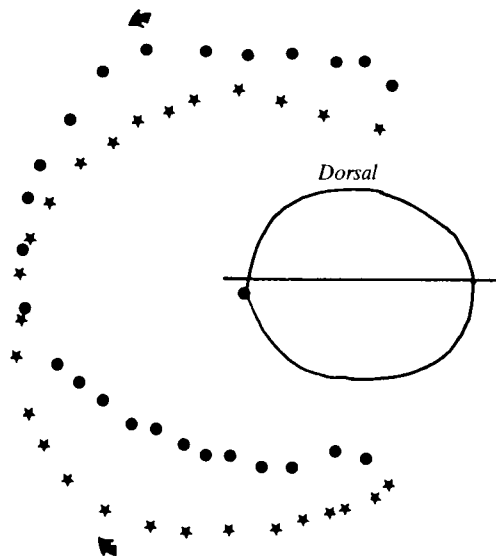


Fig. 9. Tracings of wing tip positions in oral view. Stars indicate morphological downstroke and circles, upstroke. Note that the two half-strokes are nearly identical. The horizontal line indicates the approximate location of body midline and closed circle, the point of wing attachment. Dorsal surface is uppermost. Data points are two film frames apart ($150 \text{ frames s}^{-1}$) except at the extremes of each half-stroke where a number of frames were omitted for clarity.

Clione; on the contrary, such stimuli inhibit swimming or modify the course and/or speed of locomotion. Body design is roughly streamlined in shape with a reduced foot and a lack of gills or mantle cavity. The wings are thin dorso-ventrally, but present a large surface area when fully expanded.

Pteropod wings are believed to represent highly modified parapodia (derivatives of the foot). An inspection of muscle orientation in *Clione* wings reveals that muscle layers can be favourably compared with those of the generalized gastropod foot. Longitudinal, transverse, oblique and dorso-ventral fibres can be found in varying states of development in prosobranchs (Gainey, 1976; Trueman & Brown, 1976), opisthobranchs (Brace, 1977) and pulmonates (Jones, 1973). In *Clione*, the oblique muscles are well developed and used for locomotory movements of the wings. Four layers are present, two each associated with the dorsal and ventral surfaces of the wings. Electrophysiological evidence indicates that the two dorsal layers are simultaneously active during at least part of the upstroke, just as the ventral layers are active during part of the downstroke (R. A. Satterlie & A. N. Spencer, in preparation). Oblique fibres of the typical gastropod foot are believed to produce local lifting of the sole during pedal wave propagation in pulmonates (Jones, 1973; Denny,

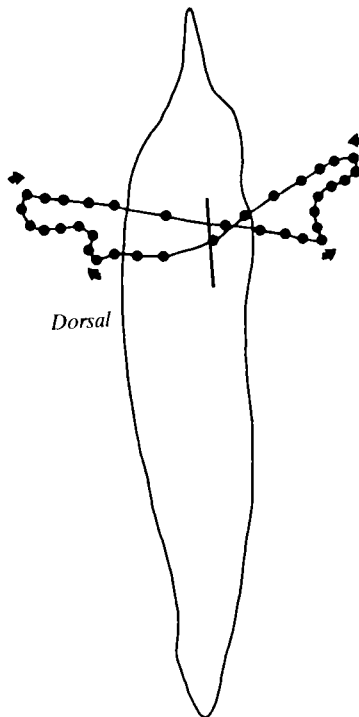


Fig. 10. Tracings of wing tip positions in side view. Arrows indicate direction of wing movement. In the latter part of each half-stroke the wing tips bend behind the rest of the wing as shown by the notches in the figure-of-eight curve. Forward movement of the wing tips is accompanied by wing stiffening, which terminates the notches. Intersection in the curve is displaced ventrally as the wings are attached nearer the ventral surface. The vertical bar indicates the position of wing attachment. Dorsal surface is to the left.

1981). In *Clione*, the longitudinal and transverse fibres function as wing retractors. It is not known if these muscles are also active during swimming. The dorso-ventral muscles of the pteropod wing presumably control wing thickness.

The seven wing muscles appear to work against a fluid skeleton, as the wings contain an extensive haemocoelic space. Blood sinuses have been described in the foot of a number of gastropods (Gainey, 1976; Jones, 1973; Trueman & Brown, 1976). High fluid pressure in sinuses is believed to contribute to the turgor required for pedal waves and forward locomotion (Denny, 1981; Jones, 1973). Trueman & Brown (1976) demonstrated that two pressure pulses coincided with extension of the foot and forward movement of the shell in the prosobranch *Bullia*. In *Clione*, an increase in the haemocoelic pressure of the body and wing cavities is presumably involved in wing inflation, since expansion is very slow relative to wing retraction. The body cavity of *Clione* is separated into cephalic and trunk haemocoels by a horizontal, muscular diaphragm. This diaphragm surrounds the anterior aorta and may act as a valve regulating blood flow to the cephalic haemocoel (Lalli, 1967). Increase in fluid pressure in the cephalic haemocoel is apparently involved in eversion of the buccal apparatus, and possibly in expansion of the wings. It is not known if the wing haemocoels are in direct contact with the cephalic haemocoel, or connected *via* valves. In any event, the fluid pressure in the two body compartments is regulated by well-developed longitudinal and circular body wall musculature. Wing thickness can be locally controlled by fluid pressure acting against dorso-ventral muscles, with the swimming muscles acting against the resulting hydrostatic skeleton.

Swimming in *Clione* was described by Morton (1958) as consisting of symmetrical sculling movements of the wings. For each wing, the upstroke and downstroke appear very similar. Wing tips nearly touch or slightly overlap at both the dorsal and ventral midlines of the body, angles of attack for upstroke and downstroke are virtually identical, and the angles of tilt of the stroke planes are similar for upstroke and downstroke. In addition, the arrangement and development of oblique muscles is identical in the dorsal and ventral surfaces of the wings. Despite these similarities, the wing tip path (Fig. 10) shows asymmetry in the figure-of-eight curve, presumably due to the ventro-lateral attachment of the wings.

Laboratory observations on freely swimming *Clione* suggest that wing movements produce lift in the formal aerodynamic sense (see Vogel, 1981) in both upstroke and downstroke. Body movements during slow swimming consist of a forward and slightly ventral lunge with each upstroke, and a forward and slightly dorsal lunge with each downstroke. The dorsal and ventral components of this lunge would be expected if lift is generated roughly perpendicular to the surface of the wing (angle of attack is 42° relative to the longitudinal body axis at wing crossover).

Wing movements during hovering swimming in *Clione* can be compared to those of hovering insects and birds. In 'normal' hovering as seen in humming-birds and insects such as coleopterans, dipterans, hymenopterans and lepidopterans (Weis-Fogh, 1973), the body is held at a steep angle relative to the vertical, and the wings beat in a horizontal plane. The wings typically rotate at the start of each beat to provide a sufficient angle of attack to generate lift.

Hovering in *Clione* matches the gross features Weis-Fogh (1973) outlined as typical of 'normal' hovering, but the low aspect ratio of the wings in *Clione* and the short length of the wing-stroke imply that the mechanism of lift generation in this animal differs from the steady-state aerodynamic mechanisms used in human technology. The same problems associated with the flight of some insects prompted Weis-Fogh (1973, 1975) to suggest two novel mechanisms for generating a circulation around the wing which is vital for lift generation; these are the 'clap-and-fling', and the 'flip'. In both mechanisms, aspects of unsteady fluid mechanics serve to create a leading edge separation vortex and initiate circulation around the wing before it has travelled any significant fraction of its chord length, thus ensuring that lift is generated by the wing throughout the stroke and avoiding the delay in lift generation typical of aerofoils started from rest (Wagner, 1925). Both theoretical (Lighthill, 1973, 1975; Edwards & Cheng, 1982) and experimental studies (Bennett, 1977; Maxworthy, 1979) have confirmed the feasibility of such mechanisms in the flight of some insects.

The 'flip' is a rapid rotation of the wing of an insect at the extreme of one half-stroke which forces the vorticity residing on the top of the wing to be relocated below the wing (Weis-Fogh, 1973; Maxworthy, 1979), ensuring downward movement of the vortex ring which surrounds the animal (Ellington, 1978; Rayner, 1979*a,b*). In *Clione*, all aspects of the wing stroke pass smoothly into the following stages and there is no sudden reversal of the surface of the wing which is uppermost nor of the stroke direction. A 'flip' mechanism is thus unlikely to be involved in lift generation.

In the 'clap-and-fling' seen in some insects (and perhaps some birds), the two wings at the top of their upstroke become appressed so that the dorsal surfaces face each other. As the downstroke begins, the anterior edges of the wings separate before the posterior edges; fluid rushes in over the anterior edges to fill the space created between the wings, in the process generating a leading edge separation vortex which allows both the immediate generation of lift with the wing stroke and a greater lift coefficient than would be possible by steady-state mechanisms (see Maxworthy, 1979, 1981). A variant of this mechanism appears to be operative in the swimming of *Clione*, but in *Clione*, the anterior margins of the wings move away from the body before the posterior margins; the space created must be filled by water flowing over the anterior edge of the wing. Presumably a leading edge separation vortex is formed, ensuring immediate lift generation and stabilizing the wings against the stall that would otherwise be likely at the high angles of attack seen in *Clione*. During the terminal *tip-forward* phase of the stroke, it seems likely that the leading edge separation vortex created during the 'fling' (*flattening* phase) is literally scraped off the upper surface of the wing and forced posteriorly, completing the downward motion of a complete vortex ring around the animal (see Ellington, 1978 and in press; Rayner, 1979*a,b*) and setting the stage for the initiation of a circulation of the opposite sense around the wing in the next half-stroke.

Maxworthy (1979), using mechanical models, demonstrated that the clap-and-fling mechanism was efficient in producing circulation around wings at Reynolds numbers as low as 32 and as high as 13000. We estimate from wing dimensions and velocity measurements that the Reynolds number of the wings in *Clione* is approximately 200,

so the proposed mechanism is physically reasonable and has some experimental support. Future work on two fronts, biomechanical and neurophysiological, are intended to determine the lift-generating mechanisms and biomechanical properties of *Clione*'s swimming structures, and to describe the cellular machinery responsible for the wing movements in electrical and morphological terms.

We thank Dr A. O. D. Willows, Director, Friday Harbor Laboratories for providing space and generous assistance, Dr R. Strathmann for the loan of the high speed movie camera, Lou and Ali Satterlie for assistance in collecting the specimens, and Dan Cantele for photographic assistance. This study was supported in part by NSERC Grant No. A0419 to ANS.

REFERENCES

- BEBBINGTON, A. & HUGHES, G. M. (1973). Locomotion in *Aplysia* (Gastropoda, Opisthobranchia). *Proc. malac. Soc. Lond.* **40**, 399–405.
- BENNETT, L. (1977). Clap and fling aerodynamics – an experimental evaluation. *J. exp. Biol.* **69**, 261–272.
- BRACE, R. C. (1977). Shell attachment and associated musculature in the Notaspidea and Anaspidea (Gastropoda; Opisthobranchia). *Trans. zool. Soc. Lond.* **34**, 27–43.
- DENNY, M. W. (1981). A quantitative model for the adhesive locomotion of the terrestrial slug, *Ariolimax columbianus*. *J. exp. Biol.* **91**, 195–217.
- EDWARDS, R. H. & CHENG, H. K. (1982). The separation vortex in the Weis-Fogh circulation-generation mechanism. *J. Fluid Mech.* **120**, 463–473.
- ELLINGTON, C. P. (1978). The aerodynamics of normal hovering flight: three approaches. In *Comparative Physiology: Water, Ions and Fluid Mechanics*, (eds K. Schmidt-Nielsen, L. Bolis & S. H. P. Maddrell), pp. 327–345. New York: Cambridge University Press.
- FARMER, W. F. (1970). Swimming gastropods (Opisthobranchia and Prosobranchia). *Veliger* **13**, 72–89.
- GABE, M. (1976). *Histological Techniques*. New York: Springer-Verlag. p. 1106.
- GAINES, L. F. (1976). Locomotion in the Gastropoda: functional morphology of the foot in *Neritina reclinata* and *Thais rustica*. *Malacologia* **15**, 411–431.
- GETTING, P. A. (1977). Neuronal organization of escape swimming in *Tritonia*. *J. comp. Physiol.* **121**, 325–342.
- GETTING, P. A. (1981). Mechanisms of pattern generation underlying swimming in *Tritonia*. I. Neuronal network formed by monosynaptic connections. *J. Neurophysiol.* **46**, 65–79.
- GETTING, P. A. (1982). Mechanisms of pattern generation underlying swimming in *Tritonia*. II. Network reconstruction. *J. Neurophysiol.* **49**, 1017–1035.
- HAMILTON, P. V. & AMBROSE, H. M. (1975). Swimming and orientation in *Aplysia brasiliana* (Mollusca: Gastropoda). *Mar. Behav. Physiol.* **3**, 131–144.
- HUGHES, G. M. (1971). An electrophysiological study of parapodial innervation patterns in *Aplysia depilans*. *J. exp. Biol.* **55**, 409–420.
- HYMAN, L. H. (1967). *The Invertebrates: Mollusca I*. New York: McGraw-Hill. pp. 471–473.
- JONES, H. D. (1973). The mechanism of locomotion in *Agriolimax reticulatus* (Mollusca; Gastropoda). *J. Zool. Lond.* **171**, 489–498.
- LALLI, C. M. K. (1967). *Studies on the Structure and Biology of Two Gymnosomatous Pteropods*, *Clione limacina Agersborg* and *Crucibranchaea machrochira (Meisenheimer)*. Ph.D. thesis, University of Washington.
- LIGHTHILL, M. J. (1973). On the Weis-Fogh mechanism of lift generation. *J. Fluid Mech.* **60**, 1–17.
- LIGHTHILL, M. J. (1975). Aerodynamic aspects of animal flight. In *Swimming and Flying in Nature*, (eds Y.-T. Wu, C. J. Brokaw & C. Brennen), pp. 423–491. New York: Plenum Press.
- MAXWORTHY, T. (1979). Experiments on the Weis-Fogh mechanism of lift generation by insects in hovering flight. Part 1. Dynamics of the 'fling'. *J. Fluid Mech.* **93**, 47–63.
- MAXWORTHY, T. (1981). The fluid dynamics of insect flight. *A. Rev. Fluid Mech.* **13**, 329–350.
- MORTON, J. E. (1958). Observations on the gymnosomatous pteropod *Clione limacina* (Phipps). *J. mar. biol. Ass. U.K.* **37**, 287–297.
- RAYNER, J. M. V. (1979a). A new approach to animal flight mechanics. *J. exp. Biol.* **80**, 17–54.
- RAYNER, J. M. V. (1979b). A vortex theory of animal flight. Part 1. The vortex wake of a hovering animal. *J. Fluid Mech.* **91**, 697–730.
- SATTERLIE, R. A. & SPENCER, A. N. (1985). Swimming in the pteropod mollusc, *Clione limacina*. II. Physiology. *J. exp. Biol.* **116**, 205–222.

- TRUEMAN, E. R. & BROWN, A. C. (1976). Locomotion, pedal retraction and extension, and the hydraulic systems of *Bullia* (Gastropoda: Nassariidae). *J. Zool. Lond.* **178**, 365–384.
- VOGEL, S. (1981). *Life in Moving Fluids*. Princeton, N. J.: Princeton University Press. 352 pp.
- VON DER PORTEN, K., REDMANN, G., ROTHMAN, B. & PINSKER, H. (1980). Neuroethological studies of freely swimming *Aplysia brasiliiana*. *J. exp. Biol.* **84**, 245–257.
- WAGNER, H. (1925). Über die Entstehung des dynamischen Auftriebes von Tragflügeln. *Z. angew. Math. Mech.* **5**, 17–35.
- WEEVERS, R. DE G. (1971). A preparation of *Aplysia fasciata* for intrasomatic recording and stimulation of single neurones during locomotor movements. *J. exp. Biol.* **54**, 659–676.
- WEIS-FOGH, T. (1973). Quick estimates of flight fitness in hovering animals, including novel mechanisms for lift production. *J. exp. Biol.* **59**, 169–230.
- WEIS-FOGH, T. (1975). Flapping flight and power in birds and insects, conventional and novel mechanisms. In *Swimming and Flying in Nature*, Vol. 2, (eds Y.-T. Wu, C. J. Brokaw & C. Brennen), pp. 729–762. New York: Plenum Press.
- WILLOWS, A. O. D. (1967). Behavioral acts elicited by stimulation of single identifiable brain cells. *Science, N.Y.* **157**, 570–574.
- WILLOWS, A. O. D. & DORSETT, D. A. (1975). Evolution of swimming behavior in *Tritonia* and its neurophysiological correlates. *J. comp. Physiol.* **100**, 117–133.
- WILLOWS, A. O. D., DORSETT, D. A. & HOYLE, G. (1973). The neuronal basis of behavior in *Tritonia*. III. Neuronal mechanisms of a fixed action pattern. *J. Neurobiol.* **4**, 255–285.
- WILLOWS, A. O. D. & HOYLE, G. (1969). Neuronal network triggering of a fixed action pattern. *Science, N.Y.* **166**, 1549–1551.